Frequency-comb-referenced mid-infrared source for high-precision spectroscopy

Jari Peltola,[1,2] Markku Vainio,[1,2] Thomas Fordell,[1] Tuomas Hieta,[1] Mikko Merimaa,[1] and Lauri Halonen[2,*]

[1]*Centre for Metrology and Accreditation, P.O. Box 9, FIN-02151Espoo, Finland*
[2]*Laboratory of Physical Chemistry, Department of Chemistry, P.O. Box 55 (A.I. Virtasen aukio 1), FIN-00014 University of Helsinki, Finland*
[*]*lauri.halonen@helsinki.fi.*

Abstract: We report on a tunable continuous-wave mid-infrared optical parametric oscillator (OPO), which is locked to a fully stabilized near-infrared optical frequency comb using a frequency doubling scheme. The OPO is used for 40 GHz mode-hop-free, frequency-comb-locked scans in the wavelength region between 2.7 and 3.4 μm. We demonstrate the applicability of the method to high-precision cavity-ring-down spectroscopy of nitrous oxide (N_2O) and water (H_2O) at 2.85 μm and of methane (CH_4) at 3.2 μm.

OCIS codes: (300.6190) Spectrometers; (300.6340) Spectroscopy, infrared; (190.4970) Parametric oscillators and amplifiers.

References and links

1. R. Holzwarth, Th. Udem, T. W. Hänsch, J. C. Knight, W. J. Wadsworth, and P. St. J. Russell, "Optical frequency synthesizer for precision spectroscopy," Phys. Rev. Lett. **85**(11), 2264–2267 (2000).
2. S. A. Diddams, L. Hollberg, and V. Mbele, "Molecular fingerprinting with the resolved modes of a femtosecond laser frequency comb," Nature **445**(7128), 627–630 (2007).
3. F. Adler, M. J. Thorpe, K. C. Cossel, and J. Ye, "Cavity-enhanced direct frequency comb spectroscopy: technology and applications," Annu Rev Anal Chem (Palo Alto Calif) **3**(1), 175–205 (2010).
4. V. Ahtee, M. Merimaa, and K. Nyholm, "Precision spectroscopy of acetylene transitions using an optical frequency synthesizer," Opt. Lett. **34**(17), 2619–2621 (2009).
5. P. Cancio, S. Bartalini, S. Borri, I. Galli, G. Garliardi, G. Giusfredi, P. Maddaloni, P. Malara, D. Mazzotti, and P. De Natale, "Frequency-comb-referenced mid-IR sources for next-generation environmental sensors," Appl. Phys. B **102**(2), 255–269 (2011).
6. S. Wojtewicz, A. Cygan, P. Maslowski, J. Domyslawska, D. Lisak, R. S. Trawinski, and R. Ciurylo, "Spectral line shapes of self-broadened P-branch transitions of oxygen B band," J. Quant. Spectrosc. Radiat. Transf. **144**, 36–48 (2014).
7. A. Schliesser, N. Picque, and T. W. Hänsch, "Mid-infrared frequency combs," Nat. Photonics **6**(7), 440–449 (2012).
8. P. Maddaloni, P. Malara, G. Gagliardi, and P. De Natale, "Mid-infrared fibre-based optical comb," New J. Phys. **8**(11), 262 (2006).
9. F. Adler, K. C. Cossel, M. J. Thorpe, I. Hartl, M. E. Fermann, and J. Ye, "Phase-stabilized, 1.5 W frequency comb at 2.8-4.8 microm," Opt. Lett. **34**(9), 1330–1332 (2009).
10. N. Leindecker, A. Marandi, R. L. Byer, K. L. Vodopyanov, J. Jiang, I. Hartl, M. Fermann, and P. G. Schunemann, "Octave-spanning ultrafast OPO with 2.6-6.1 μm instantaneous bandwidth pumped by femtosecond Tm-fiber laser," Opt. Express **20**(7), 7046–7053 (2012).
11. E. V. Kovalchuk, T. Schuldt, and A. Peters, "Combination of a continuous-wave optical parametric oscillator and a femtosecond frequency comb for optical frequency metrology," Opt. Lett. **30**(23), 3141–3143 (2005).
12. D. Mazzotti, P. Cancio, G. Giusfredi, P. De Natale, and M. Prevedelli, "Frequency-comb-based absolute frequency measurements in the mid-infrared with a difference-frequency spectrometer," Opt. Lett. **30**(9), 997–999 (2005).
13. S. Bartalini, P. Cancio, G. Giusfredi, D. Mazzotti, P. De Natale, S. Borri, I. Galli, T. Leveque, and L. Gianfrani, "Frequency-comb-referenced quantum-cascade laser at 4.4 microm," Opt. Lett. **32**(8), 988–990 (2007).
14. K. Takahata, T. Kobayashi, H. Sasada, Y. Nakajima, H. Inaba, and F.-L. Hong, "Absolute frequency measurement of sub-Doppler molecular lines using a 3.4-μm difference-frequency-generation spectrometer and a fiber-based frequency comb," Phys. Rev. A **80**(3), 032518 (2009).

#226121 - $15.00 USD Received 3 Nov 2014; revised 5 Dec 2014; accepted 5 Dec 2014; published 23 Dec 2014

15. M. Vainio, M. Merimaa, and L. Halonen, "Frequency-comb-referenced molecular spectroscopy in the mid-infrared region," Opt. Lett. **36**(21), 4122–4124 (2011).
16. I. Ricciardi, E. De Tommasi, P. Maddaloni, S. Mosca, A. Rocco, J.-J. Zondy, M. De Rosa, and P. De Natale, "Frequency-comb-referenced singly-resonant OPO for sub-Doppler spectroscopy," Opt. Express **20**(8), 9178–9186 (2012).
17. O. Asvany, J. Krieg, and S. Schlemmer, "Frequency comb assisted mid-infrared spectroscopy of cold molecular ions," Rev. Sci. Instrum. **83**(9), 093110 (2012).
18. A. A. Mills, D. Gatti, J. Jiang, C. Mohr, W. Mefford, L. Gianfrani, M. Fermann, I. Hartl, and M. Marangoni, "Coherent phase lock of a 9 μm quantum cascade laser to a 2 μm thulium optical frequency comb," Opt. Lett. **37**(19), 4083–4085 (2012).
19. K. Knabe, P. A. Williams, F. R. Giorgetta, M. B. Radunsky, C. M. Armacost, S. Crivello, and N. R. Newbury, "Absolute spectroscopy of N_2O near 4.5 μm with a comb-calibrated, frequency-swept quantum cascade laser spectrometer," Opt. Express **21**(1), 1020–1029 (2013).
20. M. Zimmermann, C. Gohle, R. Holzwarth, T. Udem, and T. W. Hänsch, "Optical clockwork with an offset-free difference-frequency comb: accuracy of sum- and difference-frequency generation," Opt. Lett. **29**(3), 310–312 (2004).
21. E. Benkler, F. Rohde, and H. R. Telle, "Endless frequency shifting of optical frequency comb lines," Opt. Express **21**(5), 5793–5802 (2013).
22. T. Fordell, A. E. Wallin, T. Lindvall, M. Vainio, and M. Merimaa, "Frequency-comb-referenced tunable diode laser spectroscopy and laser stabilization applied to laser cooling," Appl. Opt. **53**(31), 7476–7482 (2014).
23. M. Vainio, J. Peltola, S. Persijn, F. J. Harren, and L. Halonen, "Singly resonant cw OPO with simple wavelength tuning," Opt. Express **16**(15), 11141–11146 (2008).
24. C. R. Phillips and M. M. Fejer, "Stability of the singly resonant optical parametric oscillator," J. Opt. Soc. Am. B **27**(12), 2687–2699 (2010).
25. N. Bandyopadhyay, Y. Bai, S. Tsao, S. Nida, S. Slivken, and M. Razeghi, "Room temperature continuous wave operation of λ : 3-3.2 μm quantum cascade lasers," Appl. Phys. Lett. **101**(24), 241110 (2012).
26. J. Peltola, M. Vainio, V. Ulvila, M. Siltanen, M. Metsälä, and L. Halonen, "Off-axis re-entrant cavity ring-down spectroscopy with a mid-infrared continuous-wave optical parametric oscillator," Appl. Phys. B **107**(3), 839–847 (2012).
27. G. Berden, R. Peeters, and G. Meijer, "Cavity ring-down spectroscopy: experimental schemes and applications," Int. Rev. Phys. Chem. **19**(4), 565–607 (2000).
28. H. I. T. R. A. N. The, 2012 database, URL: *http://www.hitran.com/*.
29. L. S. Rothman, C. P. Rinsland, A. Goldman, S. T. Massie, S. T. Massie, D. P. Edwards, J.-M. Flaud, A. Perrin, C. Camy-Peyret, V. Dana, J.-Y. Mandin, J. Schroeder, A. McCann, R. R. Gamache, R. B. Wattson, K. Yoshino, K. V. Chance, K. W. Jucks, L. R. Brown, V. Nemtchinoy, and P. Varanasi, "The HITRAN molecular spectroscopic database and hawks (HITRAN atmospheric workstation): 1996 edition," J. Quant. Spectrosc. Radiat. Transf. **60**(5), 665–710 (1998).
30. R. Z. Martínez, M. Metsälä, O. Vaittinen, T. Lantta, and L. Halonen, "Laser-locked, high repetition-rate cavity ringdown spectrometer," J. Opt. Soc. Am. B **23**(4), 727–740 (2006).

1. Introduction

Various methods of laser absorption spectroscopy have provided techniques for fundamental studies of molecules, as well as for fast and non-intrusive trace gas analysis. Detection and composition quantification of small trace of gases in various physical, chemical, biological and industrial processes can be done with extremely high sensitivity especially in the mid-infrared (MIR) spectral region, which contains strong fundamental ro-vibrational transitions of many molecules. For example, the CH, NH, and OH stretching modes typically lead to strong absorption bands in the wavelength region between 3 and 4 μm, that is, between 2500 and 3330 cm^{-1}. The strong absorption, the large number of detectable molecules, and the relatively small absorption due to water vapor make this so-called molecular fingerprint region ideal for trace gas detection.

One of the most important technological advances in the field of laser spectroscopy has been the invention of the optical frequency comb (OFC), which provides a tool to synthesize and measure optical frequencies with extremely high accuracy [1]. This has also led to remarkable improvements in high-precision laser spectroscopy. Direct OFC spectroscopy can be used to measure large spectral spans at once [2,3], and a tunable single-frequency laser referenced to an OFC can be used to measure gas absorption lines with high resolution and accuracy [4–6]. These OFC spectroscopy methods are well-established in the visible and near-infrared (NIR) regions, the most common solutions being based on mode-locked Ti:sapphire

#226121 - $15.00 USD Received 3 Nov 2014; revised 5 Dec 2014; accepted 5 Dec 2014; published 23 Dec 2014

lasers (OFC from 0.5 to 1.1 μm) and mode-locked Er-fiber lasers (OFC from 1 to 2 μm). The extension of the mode-locked laser frequency combs to the MIR region has proven difficult [7].

Mid-infrared OFCs have been demonstrated, for example, based on difference frequency generation (DFG) [8] and synchronously pumped femtosecond optical parametric oscillators (OPOs) [9,10]. All these methods can be used to create an OFC in the molecular fingerprint region between 3 and 4 μm. An accurate single-frequency source can, in principle, be realized by referencing a narrow-linewidth mid-infrared laser to a fully stabilized MIR comb [9]. At the moment, however, the fully stabilized mid-infrared OFCs are rather complex and are not commercially available. A more common solution is to reference the MIR laser to an NIR OFC via nonlinear optical frequency conversion [11–19]. This is typically done by using continuous-wave (cw) DFG [12, 14] or a cw OPO [11, 15–17], following the scheme of Fig. 1(a). In addition, referencing of a narrow-linewidth laser to an NIR OFC by sum frequency generation (SFG) has been used at wavelengths longer than 4 μm [13, 18, 19].

Here we focus on the 3 to 4 μm region, which contains the fundamental vibrational bands of many interesting trace gas species. Figure 1(a) shows the principle of a typical cw DFG or an OPO based solution for OFC-referenced spectroscopy in this region. A high-power 1064 nm laser, such as an Nd:YAG laser or a Yb-fiber laser, is typically used as a pump source. Difference frequency generation between the 1064 nm pump laser and a tunable diode laser at ~1.6 μm produces a tunable MIR beam at ~3 μm [14]. The optical frequencies of these three beams, which are referred to as pump (p), signal (s), and idler (i), respectively, are linked to each other by the law of energy conservation:

$$\nu_p = \nu_s + \nu_i \tag{1}$$

As Eq. (1) implies, the absolute frequency of the MIR idler beam (ν_i) can be determined by measuring the frequencies ν_p and ν_s with an NIR OFC based on a mode-locked Er-fiber laser. The same method also works for a cw OPO, which is pumped at ν_p, and produces an NIR signal beam at ν_s, as well as a tunable MIR idler beam at ν_i.

An advantage of the conventional method (Fig. 1(a)) is that it cancels the carrier-envelope offset frequency (f_{ceo}) of the comb, such that only the repetition frequency f_{rep} of the comb needs to be known in order to measure the absolute frequencies ν_p and ν_s [14, 20]. However, the method is tedious to use in applications where the MIR frequency needs to be scanned, because scanning of f_{ceo} or f_{rep} of the OFC results in scanning of both ν_p and ν_s if they are locked to the OFC. This problem can be somewhat mitigated by using an electro-optic modulator for scanning only one of the offset-locked frequencies, but even then the continuous scanning range of the MIR frequency is small, typically a few tens of MHz [16]. This limited tuning range could possibly be increased by using one of the methods that have been developed for gapless [21] or nearly gapless [4, 22] scanning of offset-locked NIR lasers over more than one f_{rep}. Simple scanning of the MIR beam can also be implemented by measuring the pump and signal frequencies without locking to the comb, however at the expense of increased frequency jitter in ν_i [17].

#226121 - $15.00 USD Received 3 Nov 2014; revised 5 Dec 2014; accepted 5 Dec 2014; published 23 Dec 2014

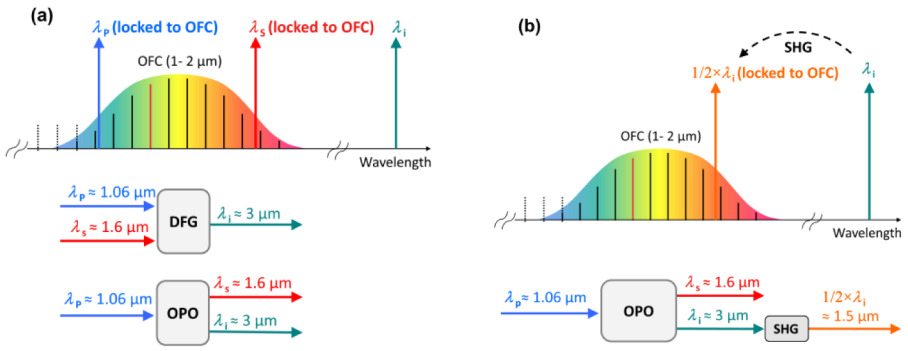

Fig. 1. (a) The absolute frequency of a mid-infrared beam produced by cw DFG or OPO can be determined by measuring the frequencies of the pump and signal beams with an NIR OFC. These frequencies are measured by counting the beat frequency with the nearest comb tooth. The optical frequency of the mth tooth of the comb is $\nu_m = f_{ceo} + mf_{rep}$, where f_{ceo} is the carrier-envelope offset frequency and f_{rep} is the repetition rate of the comb laser, both referenced to an atomic clock. The mode number m can be determined, e.g., from a coarse measurement of the respective frequency with a wavelength meter [1]. (b) The new method reported here is based on frequency doubling (second harmonic generation, SHG) of the MIR beam. This significantly simplifies the scanning of the MIR frequency ν_i while it is locked to the OFC.

Here, we report a new approach, which makes continuous scanning of the MIR frequency over a range of at least 40 GHz possible while maintaining locking to an Er-fiber laser based OFC. The principle of this approach is illustrated in Fig. 1(b). The basic idea is to frequency double the MIR beam used for spectroscopy in an MgO-doped periodically poled lithium niobate (MgO:PPLN) crystal, after which its frequency can be directly referenced to the NIR OFC. This method needs a fully stabilized OFC, i.e., also f_{ceo} needs to be known. After locking to the OFC, the frequency of the MIR beam can be tuned by scanning the repetition rate of the comb. Unlike the previous method shown in Fig. 1(a), our new method (Fig. 1(b)) does not necessarily require a parametric MIR source that fulfils Eq. (1). The frequency-doubling scheme works for any single-frequency MIR source, such as a quantum cascade laser (QCL), as long as the frequency-doubled power is sufficient for beat-frequency measurements with the OFC, and as long as the MIR wavelength is between 2 and 4 µm, such that it can be referenced to an Er-fiber-laser based OFC at 1 to 2 µm. Moreover, in contrast to previous solutions based on sum-frequency generation [13, 18, 19], our approach does not require an auxiliary high-power laser.

The details of our new method and its experimental realization are discussed in the following sections. We also demonstrate the application of the method to accurate cavity-ring-down (CRD) spectroscopy of CH_4 and N_2O/H_2O at 3.2 and 2.85 µm, respectively.

2. Experimental setup

The setup used to realize the method outlined in Fig. 1(b) is schematically shown in Fig. 2. The setup consists of three main blocks: (1) A singly-resonant cw MIR OPO, (2) a link between the MIR OPO and an NIR frequency comb, and (3) a CRD spectrometer. These blocks are discussed below in more detail.

2.1 Singly-resonant continuous-wave mid-infrared OPO

The design of the singly resonant continuous-wave OPO is similar to that reported in our previous publications [15, 23]. As a pump laser we use a narrow-linewidth Yb-fiber-laser system (IPG YAR-15K-1064-LP-SF), which produces up to 15 W of output power at 1064 nm wavelength. The pump beam is focused into a 5 cm long MgO:PPLN crystal (HC Photonics), which is placed inside the OPO cavity (Fig. 2). The temperature of the crystal can be stabilized to any value between 20 and 200 °C with a precision of ± 0.01 °C. The crystal

#226121 - $15.00 USD Received 3 Nov 2014; revised 5 Dec 2014; accepted 5 Dec 2014; published 23 Dec 2014

has seven poling periods, ranging from 28.5 to 31.5 µm. Coarse tuning of the MIR idler wavelength between 2.7 and 3.4 µm is done by changing the poling period and temperature of the crystal. Fine tuning and scanning of the idler frequency are done by the pump laser, which has a fast mode-hop-free tuning range of ~100 GHz.

The bow-tie ring cavity of the OPO is formed by four mirrors, which are highly reflective (> 99.9%) at the signal wavelength (1500-1750 nm) and transmit the pump and idler wavelengths. The rear surfaces of the mirrors are antireflection coated for all three wavelengths. The free spectral range of the cavity is ~680 MHz. To reduce the probability of mode-hops, a 0.4 mm thick solid YAG etalon is placed in the secondary focus of the OPO cavity [24]. The idler beam exiting the cavity is collimated and separated from the residual pump and signal beams using a dichroic mirror. The single-mode output power of the MIR idler beam is over 0.5 W, and the 1-second linewidth is of the order of 1 MHz.

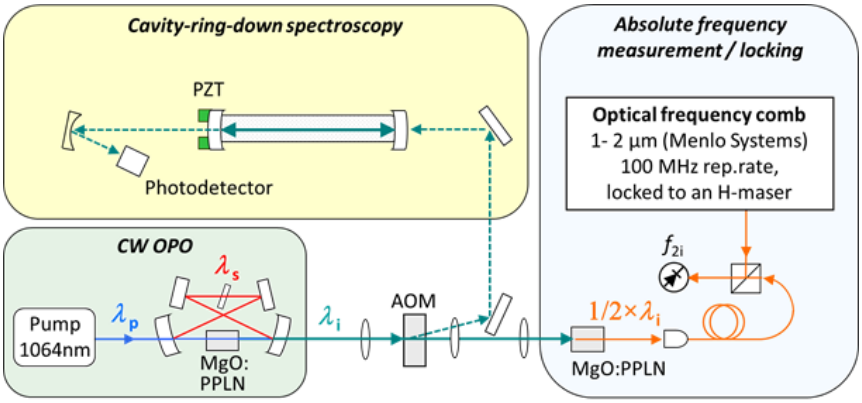

Fig. 2. A schematic picture of the experimental setup. The pump laser beam (λ_p) is coupled into a four mirror bow-tie OPO cavity. The mirrors are highly reflective for the signal beam (λ_s). A fraction of the MIR output beam (λ_i ~3 µm) is directed to a cavity-ring-down setup for sensitive molecular spectroscopy. The absolute frequency of the beam is measured with an NIR frequency comb after frequency doubling in a nonlinear crystal. The same setup can also be used to lock the MIR frequency to the OFC, after which it can be scanned by scanning the OFC. The symbol AOM denotes an acousto-optic modulator used to initiate ring-down events. MgO:PPLN is a nonlinear optical crystal. The symbol PZT denotes a piezoelectric actuator.

2.2 Link between the MIR OPO and an NIR frequency comb

The MIR output beam of the OPO is frequency doubled in order to link it to an NIR frequency comb according to the scheme outlined in Fig. 1(b). To do this, the MIR beam is focused into a 20 mm long frequency-doubling crystal (MgO:PPLN). The calculated $1/e^2$ waist size of the focused MIR beam in the middle of the crystal is 60 µm. The crystal has 6 poling periods with a 0.4 µm step increment between 33.3 and 35.3 µm, and antireflection coated end facets. The crystal is placed in an oven, whose temperature can be set between 20 and 200 °C. The available poling periods and temperature tuning range allow frequency doubling of any MIR wavelength between 2.7 and 3.4 µm.

The frequency-doubled idler beam is guided through an optical fiber link to a beat-frequency measurement with a commercially available, fully stabilized OFC (Menlo Systems FC1500-100). The OFC covers wavelengths between 1 and 2 µm directly, and has a repetition rate of 100 MHz. The repetition rate and the offset frequency of the OFC are referenced to an active hydrogen maser, which is traceable to the SI-second. The OFC output is filtered twice with a diffraction grating (Thorlabs GR25-0613), and subsequently combined with the frequency-doubled idler beam of the OPO using a single mode fiber combiner with a 50/50 split ratio. The beat signal between the combined beams is detected using a fast fiber-coupled

#226121 - $15.00 USD Received 3 Nov 2014; revised 5 Dec 2014; accepted 5 Dec 2014; published 23 Dec 2014

InGaAs detector. The beat frequency is counted with a frequency counter (Menlo Systems FXM50).

The OPO MIR frequency is locked to the OFC using a simple method: the beat note between the frequency-doubled idler beam and the OFC is read with the frequency counter, and this beat frequency is stabilized to a pre-set value by applying a correction to the OPO pump laser frequency (which, according to Eq. (1), leads to an equally large correction in the idler frequency). We typically lock the beat frequency to 20 MHz, and filter the beat signal with a 48 MHz low-pass filter before the counter. The correction signal is obtained from a proportional-integral (PI) controller implemented with LabVIEW (National Instruments). The bandwidth of the PI control is a few tens of hertz, which is limited by the shortest available gate time (4 ms) of the frequency counter. The effect of this stabilization method on the MIR idler frequency is demonstrated in Fig. 3. It is worth noting that true phase locking and faster feedback are also possible, which would reduce the linewidth of the OFC-locked OPO. However, in this work, we deliberately used the counter-based frequency-locking method, because it is simple to implement and use, and provides sufficient frequency stability for sub-Doppler spectroscopy, as is discussed in Section 3.

With the frequency locking applied, the scanning of the MIR frequency of the OPO is done by adjusting the repetition rate of the OFC. The repetition rate can be changed in total by 430 kHz using a stepper motor and a piezoelectric actuator. At the center wavelength 1560 nm of the comb, the mode number m is ~1 900 000. Therefore, the full range of repetition rate tuning corresponds to an (optical) frequency tuning of $m \times 430$ kHz = ~820 GHz, which corresponds to a maximum continuous tuning of 820 GHz/2 = 410 GHz in the MIR region. In our case, the mode-hop-free scanning range of the MIR frequency of the OFC-locked OPO is in practice limited to 100 GHz, which is the tuning range of the OPO pump laser. Any frequency scan larger than this requires a change in the temperature and/or poling period of the OPO crystal, and subsequent relocking to the OFC.

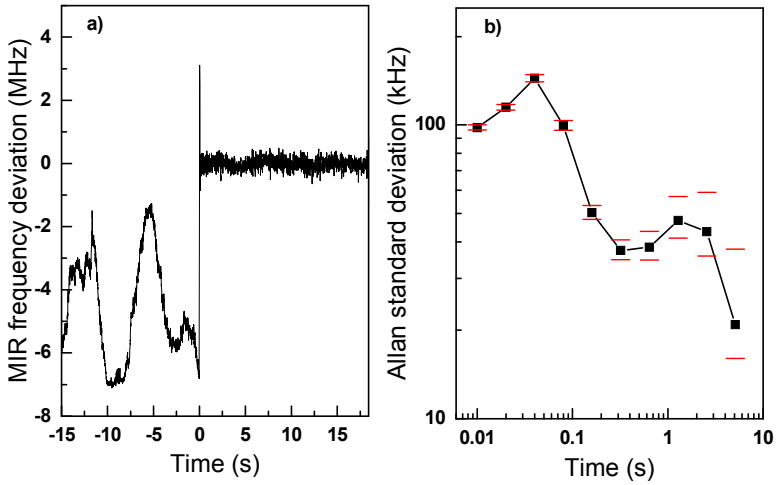

Fig. 3. a) OPO idler frequency jitter as derived from an SHG beat frequency measurement. The OPO is free-running before 0 s and locked to the OFC after 0 s. b) Allan deviation of the OFC-locked OPO frequency calculated from Fig. 3(a).

A beat signal signal-to-noise ratio (SNR) of approximately 25 dB (with 300 kHz resolution bandwidth, RBW) is needed for reliable frequency counting and locking. Owing to the irregular envelope spectrum of the OFC, the required frequency-doubled power depends on the wavelength, but in general the 25 dB SNR can be obtained with our experimental setup

#226121 - $15.00 USD Received 3 Nov 2014; revised 5 Dec 2014; accepted 5 Dec 2014; published 23 Dec 2014

if the frequency-doubled power exceeds 10 μW at the photodetector which is used for beat frequency counting. Figure 4 shows the theoretical and measured frequency-doubled power as a function of the MIR power entering the 20 mm long MgO:PPLN crystal. With an optimized frequency doubler, the required beat-note SNR can be obtained with an MIR power of as low as 100 mW. This suggests that the same method could also be applied with other MIR laser sources, such as quantum cascade and interband cascade lasers, which are also rapidly developing in the 3 to 4 μm region with a promise of high cw output power and broad tuning range [25]. It is worth noting that the frequency-doubling efficiency can be further improved by, e.g., using a longer MgO:PPLN crystal, an MgO:PPLN waveguide, or by placing the crystal in a power build-up cavity.

In practice, we observe a frequency-doubling efficiency which is 40-50% of the theoretical maximum (Fig. 4(a)). This is attributed to mainly optical losses due to imperfect coatings of the crystal ends and the dichroic mirrors that are used to separate the frequency-doubled beam from the MIR beam. With 0.5 W of MIR power, we typically measure 80-90 μW of frequency-doubled power. After losses due to the fiber combiner and a 50 m optical fiber link that connects the OPO laboratory and the OFC laboratory, we obtain, depending on the wavelength, a 25 to 40 dB SNR in the beat frequency measurement with the comb (300 kHz RBW). The phase-matching curve of the doubling crystal is more than 200 GHz wide even for the long-wavelength end of the MIR tuning range (Fig. 4(b)), which means that the continuous OFC-locked scans extending over 100 GHz can easily be done without changing the temperature or poling period of the crystal.

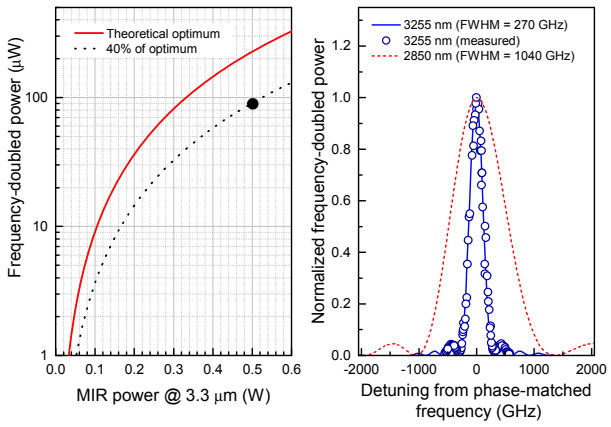

Fig. 4. (a) Frequency-doubling efficiency using a 20 mm long MgO:PPLN crystal with optimal focusing of the MIR beam. The curves show the calculated frequency-doubled power as a function of the MIR power, and the dot indicates a measured power. (b) Phase-matching curves at two different MIR wavelengths, 2850 and 3255 nm.

2.3 Cavity-ring-down spectrometer

The OFC-locked MIR OPO presented above can be combined with any standard absorption spectroscopy method, such as direct absorption spectroscopy, wavelength modulation absorption spectroscopy, and cavity-enhanced spectroscopy. In addition, the high MIR output power of the OPO makes the setup suitable for saturated-absorption spectroscopy and photo-acoustic spectroscopy. In this work, we demonstrate the applicability of the instrument in CRD spectroscopy. The CRD spectrometer is briefly described below.

As is schematically shown in Fig. 2, a small fraction of the MIR output power of the OPO is directed to a ring-down cavity in on-axis configuration. If high MIR power is needed for spectroscopy, one can also use the 0.5 W MIR beam passing through the frequency-doubling

#226121 - $15.00 USD Received 3 Nov 2014; revised 5 Dec 2014; accepted 5 Dec 2014; published 23 Dec 2014

crystal, since the depletion of this beam due to the doubling process is negligible. The ring-down cavity is formed by two highly reflecting concave mirrors, which each has a radius of curvature of 1 m. The mirrors are placed on commercial mirror holders (Los Gatos) and connected with each other by a 0.5 m long stainless-steel tube. In our experiments, we have used two mirror sets: The first set has a reflectivity of about 0.9994 at 3.2 μm, which corresponds to a ring-down time of ~3 μs [26]. The second set of mirrors has a reflectivity and ring-down time of 0.9997 and ~8 μs, respectively, at 2.85 μm. The MIR beam leaking out of the cavity is focused by a 10 cm lens on a fast photodetector (Vigo system, PVI-2TE-5/VPDC-20I). The ring-down signal from the detector is processed and digitized by a fast 14 bit data acquisition card (Gage, Compuscope 14100), and subsequently fitted by the least-squares method to a single exponential function using the Levenberg–Marquadt algorithm in a LabVIEW program.

The ring-down events are initiated by switching off the MIR beam incident on the ring-down cavity using an acousto-optic modulator (AOM) after the optical power inside the cavity reaches a certain trigger level. At every measured frequency point, the ring-down cavity frequency is matched to the OFC locked frequency by modulating the length of the cavity using piezoelectric actuators. The modulation frequency is typically 10 to 30 Hz. The measurements of the ring-downs are synchronized with the OFC-measurement of the MIR frequency. In addition, the 50 MHz signal driving the AOM can be referenced to the same time base (hydrogen maser) as the OFC, in order to accurately account for the nominal 50 MHz frequency shift that the AOM causes to the MIR beam, which is directed to the CRD-measurement. Even when the AOM is not referenced to the maser, the observed frequency jitter/drift of the AOM frequency is negligibly small, of the order of 1 Hz/h.

3. Application to high-precision absorption spectroscopy

We have used the frequency-comb referenced MIR spectrometer of Fig. 2 for high-precision spectroscopy of N_2O, H_2O, and CH_4. As an example, Fig. 5(a) shows a continuously scanned spectrum of an N_2O sample at 2.85 μm in the presence of water, demonstrating a large (40 GHz) mode-hop-free scan of the spectrometer while maintaining locking to the OFC. The 40 GHz mode-hop-free tuning range makes the setup useful for the measurements of several transitions in a single scan in the wavelength region below 4.0 μm. The measurement presented in Fig. 5(a) took approximately one hour, but much faster scanning speed can be obtained without locking the OPO to the comb, as has been demonstrated by Knabe et al. using a comb referenced external-cavity QCL at 4.5 μm [19]. Meanwhile the locking to the OFC ensures accurate calibration of the frequency axis, the vertical axis (absorbance or absorption coefficient) is also accurately calibrated thanks to the CRD-technique used in the measurement [27]. This combination of accurate measurement of both absorbance and frequency axis is useful, e.g., for measurements of molecular absorption line parameters in attempt to improve the accuracy of spectroscopic databases, such as HITRAN [28].

Measurement of absorption line intensities is an example of an application that requires high accuracy of both frequency and absorbance. The line intensity S_T can be calculated from the integrated absorption coefficient [29]. Figure 5(b) shows, as an example, a measurement of the line intensity of the R44e transition of the $\nu_1 + \nu_3$ band of N_2O. Each frequency point (black marker) in the spectrum is an average of 50 ring-down events recorded during 5 s. The line intensity deduced from the measurement is $S_0 = 2.7472 \times 10^{-21}$ $cm^{-1}/(molecule/cm^{-2})$, which is close to the value listed in the HITRAN database ($S_0 = 2.7540 \times 10^{-21}$ $cm^{-1}/(molecule/cm^{-2})$, with a stated uncertainty of 2 to 5%) [28]. The noise-equivalent absorption sensitivity calculated from the residual of the line intensity measurement is 9.8×10^{-8} cm^{-1} $Hz^{-1/2}$. The estimated total uncertainty of our line intensity is 3.4%, mainly limited by the fitting procedure (3.0%). The line-intensity data were fitted using both Voigt and Galatry profiles with no significant difference in the residuals, see Fig. 5(b). This might indicate that there are other disturbing mechanisms than Dicke narrowing, such as speed-

#226121 - $15.00 USD Received 3 Nov 2014; revised 5 Dec 2014; accepted 5 Dec 2014; published 23 Dec 2014

dependent effects. Alternatively, the SNR of the measurement (~100) is not high enough to reliably fit a Galatry profile. The statistical uncertainty of the ring-down fitting is 0.3%. The uncertainties due to the mole fraction, temperature, and pressure gauge are 1.5, 0.3, and 0.2%, respectively.

In general, with our new method, we can precisely measure the line center frequencies, line shapes, broadening, as well as the line intensities. As the OPO is locked to the OFC, the scans can be performed slowly to take advantage of averaging, without the fear of compromising the frequency accuracy due to drifting of the OPO frequency.

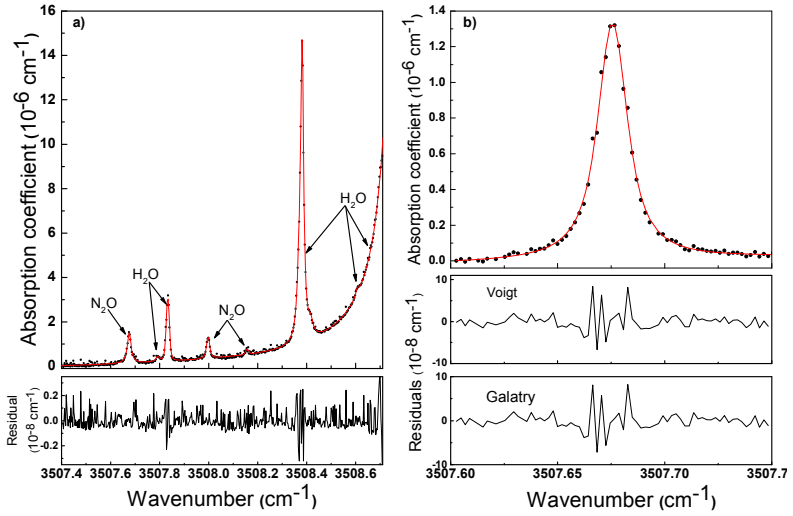

Fig. 5. (a) A continuous scan of 40 GHz measured with a frequency comb locked OPO. Red line is the least-square Voigt fit to the measured data points (black markers). Below the spectra is the residual of the fitted model. Pressure was 100 mbar. (b) The R44e transition of the $\nu_1 + \nu_3$ band of N_2O at the pressure of 100 mbar. Black markers in the spectra present measured data points and the red line presents the least-square Voigt and Galatry fits to them. Below the spectra are the residuals of the fitted models. The nitrous oxide mixing ratio was 5 ppmv ± 1.5%.

The high finesse of the ring-down cavity leads to high intracavity power even at modest input powers. In our experiments, we send 10 to 100 mW of MIR power into the ring-down cavity and typically couple it with ≥10% efficiency. This means that even at 3.2 μm, where the empty-cavity finesse is approximately 5200, we can easily reach watt-level cw power circulating in the cavity. This power is sufficient to saturate the strong fundamental ro-vibrational transitions of many molecules within the tuning range of the spectrometer. Here, we demonstrate saturated CRD spectroscopy by measuring R8 transition of the ν_3 band of methane at 3.2 μm. As is shown in Fig. 6(a), many of the tetrahedral components of this transition are overlapping even at low pressures where pressure broadening is small and the lines are only about 150 MHz wide owing to Doppler broadening. The saturation of the absorption allows us to carry out measurements with sub-Doppler resolution, which significantly improves the precision in determining the absorption line centers, especially in the case of overlapping lines. Figure 6(b) shows an example of a Lamb dip (saturated absorption feature) of one of the tetrahedral components. The high spectral resolution at the center of the transition is achieved by scanning the repetition rate of the OFC in steps of ~0.5–1.0 Hz (~0.5-1.0 MHz in the mid-IR). In the wings of the transition, the frequency step is larger.

#226121 - $15.00 USD Received 3 Nov 2014; revised 5 Dec 2014; accepted 5 Dec 2014; published 23 Dec 2014

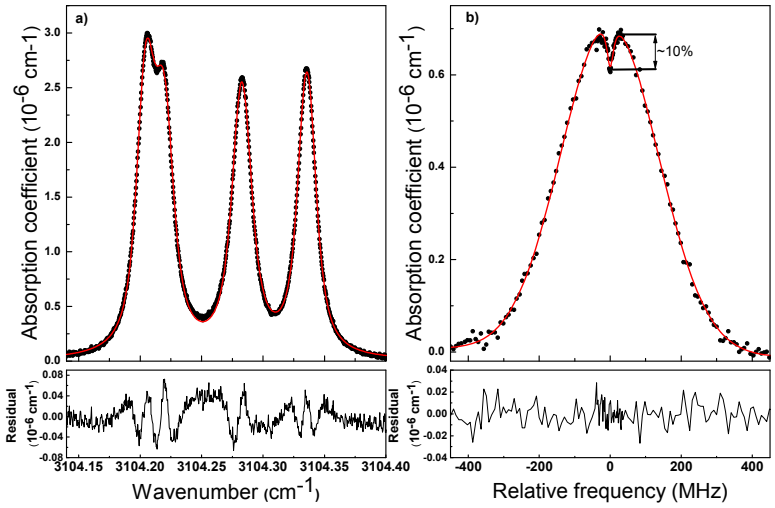

Fig. 6. (a) A part of the spectrum of the R8 transition of the ν_3 band of CH_4 at the pressure of 50 mbar. (b) A spectrum of a Doppler broadened $F_1^{(2)}$ R8 component of CH_4 with a Lamb dip at the center of the transition at the pressure of 1 mbar. Red lines are least-square Voigt fits to the measured spectra. Below the spectra are the residuals of the fitted model. The methane mixing ratio was approximately 5 ppmv.

4. Conclusion

In this article, we have reported a new method that can be used for high-resolution OFC-referenced spectroscopy in the mid-infrared region. The method is based on frequency doubling of the MIR beam used for spectroscopy, after which it can be referenced to a commercially available, fully stabilized Er-fiber-laser OFC in the NIR region, thus circumventing the problem of lacking MIR frequency combs. Here, we have demonstrated implementation of the method using a singly-resonant cw OPO as the coherent MIR light source, which is referenced to an Er-fiber-laser OFC. In the future, the method can also be used with other cw lasers that are tunable in the MIR region, between 2 and 4 μm, which is the region for which the doubled frequency overlaps with the span of the Er-fiber-laser OFC. Approximately 100 mW of MIR laser power is needed when using a simple single-pass frequency doubling scheme. This power level will likely be within the capabilities of cw interband cascade lasers and quantum cascade lasers in the near future [25].

We have used the new method for high-precision, sub-Doppler spectroscopy of N_2O/H_2O and CH_4 at 2.85 and 3.2 μm, respectively. We have experimentally demonstrated that the method can be used for large, 40 GHz mode-hop-free scans while maintaining locking of the MIR frequency to the OFC. The accuracy of the frequency axis calibration in these measurements was approximately 50 kHz (1 s averaging time), which was limited by the relatively small (a few tens of hertz) locking bandwidth used to stabilize the MIR OPO to the OFC. The locking bandwidth was limited by the frequency counter, which was used as a part of the locking circuitry to keep the experimental setup simple and versatile. For applications that require even better frequency accuracy, further improvements can be obtained by increasing the locking bandwidth and by using a phase-locked loop, which is a standard technique for laser stabilization to an OFC [1, 4]. The accuracy of cavity-ring-down-spectroscopy can be improved by stabilizing the ring-down-cavity length by locking the laser to it [6, 30].

#226121 - $15.00 USD Received 3 Nov 2014; revised 5 Dec 2014; accepted 5 Dec 2014; published 23 Dec 2014

Acknowledgments

This work is supported by the European Metrology Research Programme (Contract No. ENV-06). The EMRP is jointly funded by the EMRP participating countries within EURAMET and the European Union. The financial support of the University of Helsinki and the Academy of the Finland is gratefully acknowledged.

#226121 - $15.00 USD Received 3 Nov 2014; revised 5 Dec 2014; accepted 5 Dec 2014; published 23 Dec 2014